Journal of Materials Processing Technology 149 (2004) 172–177

Journal of Materials Processing Technology

www.elsevier.com/locate/jmatprotec

Series–parallel resonant converter for an EDM power supply

Rosario Casanueva*, Francisco J. Azcondo, Salvador Bracho

Department of Electronics Technology, Systems and Automation Engineering, University of Cantabria, Avda. de los Castros, s/n, 39005 Santander, Spain

Accepted 20 October 2003

Abstract

A new EDM impulse generator based on a HF-switched dc to dc series–parallel resonant converter is presented. The converter generates the necessary voltage, first to ionize the dielectric and then to maintain the discharge and, provided that it operates in constant current mode, the impulse generator has inherent short-circuit protection. As the switches turn on at zero voltage the converter presents minimum switching losses. The characteristics of this power electronic system are high speed control of the quality of each pulse, small size and light weight suitable for on-site machining.

The EDM power supply has been validated to perform operations in a nuclear power plant application. The design and results are described in this paper.

Keywords: Electrical discharge machining; EDM impulse generator; Resonant converter

1. Introduction

Electrical discharge machining is frequently used to provide maintenance and reparation services in nuclear power plants where EDM is a suitable process for performing machining tasks because it does not produce chips. In EDM, micron-sized particles are immediately flushed away with the dielectric fluid. In addition, it can be operated underwater and remotely which reduces personnel radiation exposure [1,2].

The power supply of EDM systems for field operation should ideally be small and light for portable on-site machining. US patents [3–5] describe electrical discharge machining tools for performing EDM operations in nuclear plants which are focused on the mechanical system and only briefly mention the use of a commercial power supply [3] or suitable power supplies [4,5].

At present, the development of EDM impulse generators is determined by their power dissipation and size reduction and by the needs of specific EDM applications [6,7]. Most of the power supply circuits in the patent literature use well-known topologies adapted to this process and differences are found in the way to control them for EDM applications.

Other well-known circuits are resonant converters. Advances in power electronics target smaller, lighter, more efficient, less expensive and more reliable energy sources. The increase of operation frequency to reduce the size of magnetic components leads to higher switching losses. High-frequency resonant converters allow power semiconductor operation with reduced switching losses [8,9]. A large number of works have been published in recent years on resonant power conversion because it meets the needs of a wide range of applications such as arc welding, electronic ballasts for lamps, induction heating, dc–dc converters, etc.

2. EDM power supply

As mentioned, the requirements of the power supply are small size and light weight and suitability for portable on-site machining. Also, since changes in the gap distance may lead to load changes from open- to short-circuit conditions, EDM has the basic requirement of limiting both the load current under short-circuit conditions and the load voltage under open-circuit conditions. The breakdown and channel formation phase presents a negative dynamic impedance so that a power converter operating in current mode (high impedance) is preferred for the utility line to see overall positive impedance.

The designed EDM impulse generator is a full-bridge series–parallel (LC_sC_p) resonant converter, shown in Fig. 1, whose switching frequency is much higher than the machining frequency.

* Corresponding author. Tel.: +349-42200872; fax: +349-42201873.
E-mail address: charo@teisa.unican.es (R. Casanueva).

0924-0136/$ – see front matter © 2004 Published by Elsevier B.V.
doi:10.1016/j.jmatprotec.2003.10.038

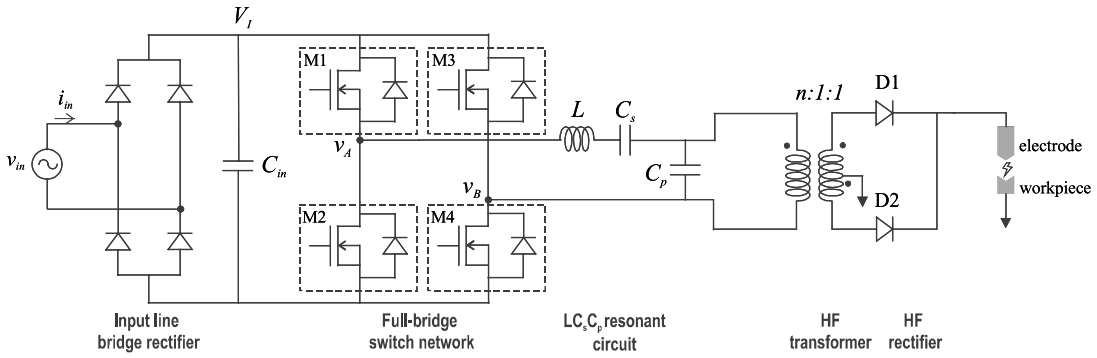

Fig. 1. Circuit diagram of the EDM power supply using a full-bridge LC_sC_p resonant converter.

LC_sC_p resonant converters are able to achieve the required overvoltage for the dielectric breakdown and, working above the resonant frequency, current lags voltage so that this topology achieves zero voltage switching (ZVS), that is, transistors turn-on at zero voltage, resulting in minimum switching losses. The full-bridge configuration has been chosen because of its capability of converting high power.

The design sequence of the LC_sC_p resonant inverter is oriented to achieving the dielectric breakdown and current stabilization while limiting maximum stress on the components by design.

2.1. Power supply description

As shown in Fig. 1 the proposed power supply consists of the following blocks:

- Input stage: it includes a single-phase bridge rectifier and a filter capacitor C_{in} to generate the inverter input voltage, V_I, from the utility line voltage. A power factor controller can also be used to improve the input stage performance regarding the harmonic injection in the utility line.
- Inverter stage: the full-bridge inverter produces a high-frequency square-wave voltage, v_{AB}. The switches are low-cost MOSFETs.
- Resonant stage: the purpose of the resonant circuit is to filter the output voltage of the inverter, v_{AB}, to obtain sinusoidal voltage and current waveforms at the load. The resonant tank must provide the necessary steady-state load voltage and current with minimum resonant current to reduce switching losses.
- Transformer: it reduces the input voltage to supply the gap with the required voltage; the transformer turn ratio is established according to the maximum output voltage of the resonant tank and the breakdown voltage.
- Output stage: it is a high-frequency full-wave rectifier consisting of hyperfast diodes with soft recovery characteristics to reduce recovery losses. No output filter is used to minimize cost and weight, although it could be used to reduce the ripple.
- Control circuit (not shown in Fig. 1): performs several functions, such as:
  - Generation of MOSFET switching signals.
  - Overvoltage protection.
  - Short-circuit and arc detection and suppression, if desired.

2.2. Operation principle

Fig. 2(a) shows the full-bridge series–parallel resonant inverter, which consists of four MOSFETs and the resonant network $LC_sC_pR_i$, where R_i is the equivalent resistance that models the transformer, the output rectifier and the gap. The transistors are driven by square-wave voltages v_{gs1}, v_{gs2}, v_{gs3} and v_{gs4}, which establish the conduction of M1 and M4 alternately to the conduction of M2 and M3, so that the full-bridge topology applies a square-wave voltage, v_{AB}, to the resonant network.

The waveforms in the resonant circuit are nearly sine waves, so essentially a sine wave appears at v_{AB}. This analysis method is called the fundamental approximation [4], and the inverter is simply represented by the first harmonic of v_{AB} as shown in Fig. 2(b).

The equivalent impedance, Z_i, across the AB terminals determines the operation mode. At the resonant frequency of the $LC_sC_pR_i$ tank, ω_r, this impedance is purely resistive and the resonant current, i_L, is in phase with v_{AB1}. For $\omega < \omega_r$, the series–parallel circuit represents a capacitive load, hence the current i_L leads v_{AB1}, and for $\omega > \omega_r$, the resonant circuit represents an inductive impedance and the current i_L lags the voltage v_{AB1}, so transistors turn on at zero voltage as shown in Fig. 3 and switching losses are null. This operation mode, known as zero voltage switching, is chosen for the EDM power supply.

2.3. Series–parallel resonant inverter analysis

The analysis of the simplified circuit is based on the following parameters:

- the equivalent resistance, R_i;
- the ratio of the series and parallel capacitance, $A = C_p/C_s$;
- the parallel parameters, given in Table 1.

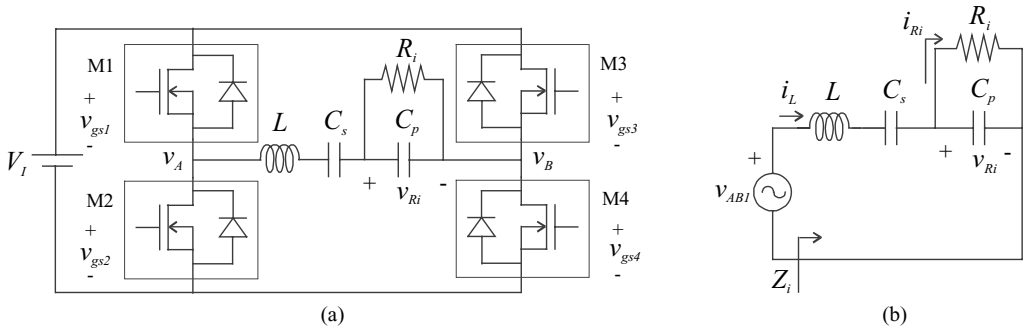

Fig. 2. (a) Full-bridge LC_sC_p resonant inverter and (b) simplified model.

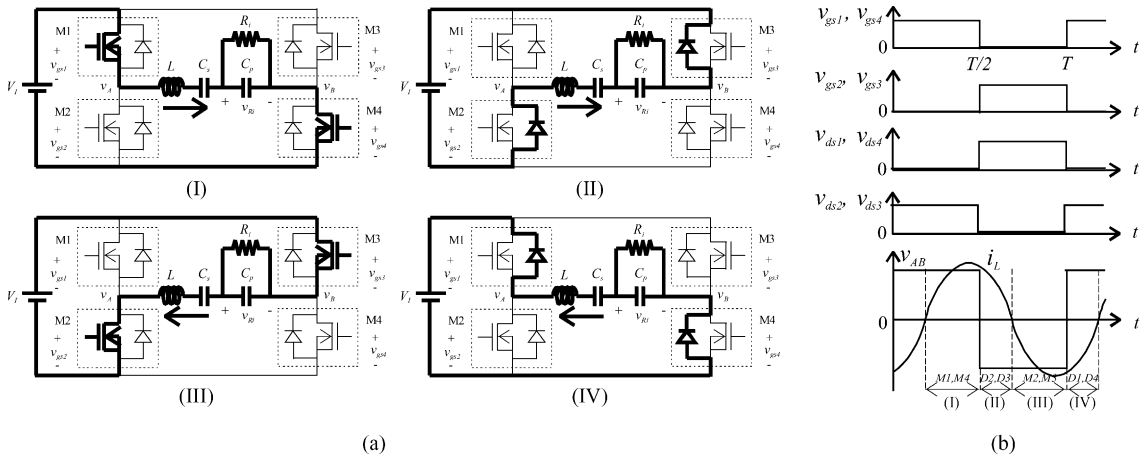

Fig. 3. (a) Switching sequence and (b) circuit waveforms for ZVS operation mode.

The modulus of the voltage gain is

$$\frac{\hat{V}_{\mathrm{R_i}}}{\hat{V}_{\mathrm{AB1}}} = \frac{1}{\sqrt{[A+1-k^2]^2 + \frac{1}{Q_\mathrm{p}^2}\left[k - \frac{A}{k}\right]^2}} \tag{1}$$

and it is shown in Fig. 4(a) as a function of the normalized switching frequency $\mathrm{K} = \omega/\omega_\mathrm{p}$ for different values of parallel quality factor that represent the load conditions in the gap.

To design the resonant inverter as a current source, the expression of the current amplitude through the equivalent resistance is analyzed:

$$\hat{I}_{\mathrm{R_i}} = \frac{4V_\mathrm{I}}{\pi Z_\mathrm{p} Q_\mathrm{p}} \sqrt{\frac{1+Q_\mathrm{p}^2 k^2}{1+\left[\frac{1}{Q_\mathrm{p}}\left(k-\frac{A}{k}\right)(1+Q_\mathrm{p}^2k^2) - Q_\mathrm{p}k\right]^2}} \tag{2}$$

Table 1
LC_sC_p parallel parameters

Resonant frequency	$\omega_\mathrm{p} = \dfrac{1}{\sqrt{LC_\mathrm{p}}}$
Characteristic impedance	$Z_\mathrm{p} = \omega_\mathrm{p} L = \dfrac{1}{\omega_\mathrm{p} C_\mathrm{p}}$
Quality factor	$Q_\mathrm{p} = \dfrac{R_\mathrm{i}}{Z_\mathrm{p}}$

Fig. 4(b) shows the normalized current as a function of the frequency for different parallel quality factors, that is, for different loads. Expression (2) has no dependence on the load at the frequency

$$\omega = \omega_\mathrm{p}\sqrt{A+1} = \omega_0 \tag{3}$$

where ω_0 is the unloaded natural resonant frequency of the LC_sC_p circuit.

Thus, at this frequency, the current amplitude through the equivalent resistance for any value of R_i becomes

$$\hat{I}_{\mathrm{R_i}}|_{\omega=\omega_0} = \frac{4V_\mathrm{I}}{\pi Z_\mathrm{p}}\sqrt{1+A} \tag{4}$$

The current source behavior guarantees the gap current stability, so this frequency, ω_0, is chosen as the fixed switching frequency. At this frequency, the voltage gain (1), shown in Fig. 4(a), is reduced to the expression

$$\left.\frac{\hat{V}_{\mathrm{R_i}}}{\hat{V}_{\mathrm{AB1}}}\right|_{\omega=\omega_0} = Q_\mathrm{p}\sqrt{A+1} \tag{5}$$

So, for high Q_p the voltage gain is enough to achieve the dielectric breakdown. Although expression (5) also implies that for an open-circuit condition, $Q_\mathrm{p} \to \infty$, the voltage gain would be infinite, so the maximum value of the voltage gain must be limited by an overvoltage protection.

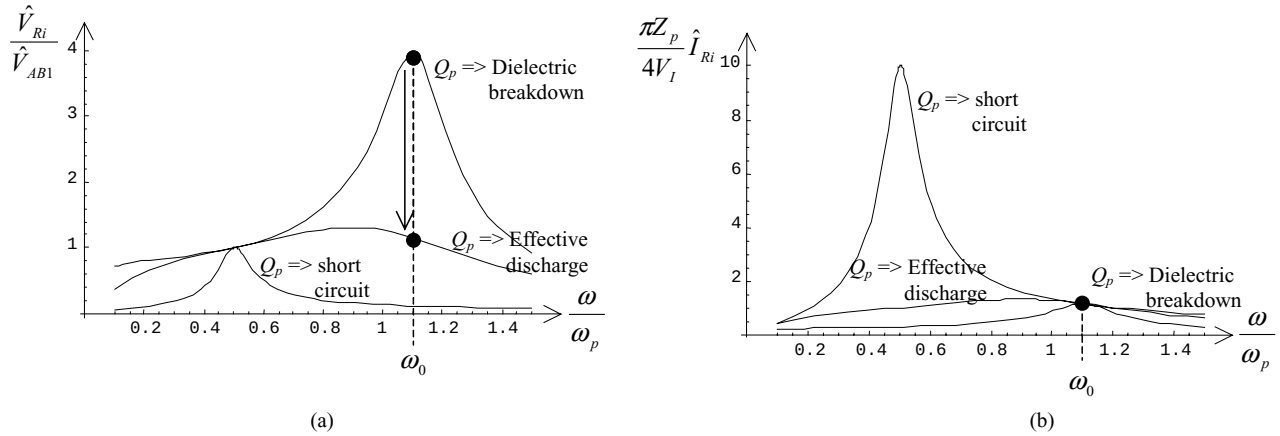

Fig. 4. LC_sC_p circuit (a) voltage gain and (b) normalized output current ($A = 1/4$).

From the operation principle and the inverter analysis, a design sequence of the current source series–parallel resonant converter has been established. Also, sensitivity and Monte Carlo analysis have been performed to study the effects of the tolerance of circuit elements in order to optimize the design parameters that ensure the circuit performance and repeatability with no feedback.

3. EDM control

Fig. 5 shows the simplified block diagram of the system that controls the EDM process. Two different controls are distinguished: the power supply control and the stepper motor control. The power supply performs on-line suppression of the undesired action of unwanted pulses, whereas the feed system response time is in the millisecond range, so it cannot react to single pulses.

3.1. Gap sensor and signal conditioning

The gap voltage is monitored and scaled down. The resulting magnitude is filtered in order to remove unwanted noise for the power supply control and to obtain the average gap voltage for the stepper motor control.

Threshold voltages are used to compare the sampled gap voltage to detect arcs, shorts and open circuits, resulting in the *arc*, *cc* and *ov* signals, respectively. In the same way, threshold voltages are established to maintain the adequate gap width; the average gap voltage is compared to these thresholds to obtain the *up* and *down* signals that control the stepper motor movement.

3.2. Power supply control

The control circuit is implemented by means of a CPLD, which allows easy modification of the design, clocked by a 20 MHz crystal oscillator. The power supply control establishes the switching frequency of the resonant inverter slightly above the natural resonant frequency, f_0, to fix the desired output current during the machining pulse on-time. During the off-time, power switches are turned off. This control circuit generates the drive signals to the power MOSFETs at the desired frequency.

Signal v_{ref}, which is a pulse-width-controlled signal at 10 kHz, the specified machining frequency, sets the on-time and the off-time. If the overvoltage protection is activated during the on-time, the power MOSFETs are turned off until the next machining pulse. The same action can be forced if an arc or short circuit is detected to prevent damage to the workpiece and excessive wear in the electrode.

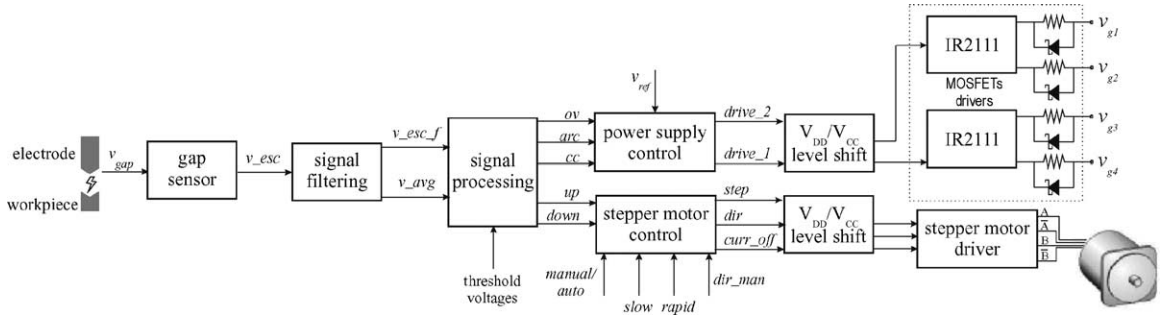

Fig. 5. EDM process control.

Since the switching frequency control is precise, no feedback control is required, preventing the system from any feedback control lag and noise injection. Results of Monte Carlo simulations support this choice.

3.3. Stepper motor control

This circuit reacts under open-circuit and short-circuit conditions, moving the electrode downwards and upwards, respectively. The gap width control circuit is also implemented in a CPLD. The motor is an MAE stepper motor model HY 200 2226 0250 AX 06, and is driven by a RTA stepper motor driver model GMD 02. The control provides two operation modes: manual and automatic.

A manual operation allows an operator to move the electrode up or down, according to the indication of the direction signal, *dir_man*. The movement can be chosen to be slow or fast by means of *slow* and *rapid* signals.

In the automatic operation mode, the sampling period is 10 ms. Depending on the state of the *up* and *down* signals, the stepper motor driver inputs, *step*, *dir* and *curr_off*, are generated. *Curr_off* input enables or disables the driver. *Dir* establishes the motor rotation direction and, if the driver is active, the *step* input generates a single step each sampling period.

4. Experimental results

The circuit has been verified by practical EDM experiments on different metal workpieces. Fig. 6 shows the transistors switching current and voltage, the reference voltage, v_{ref}, changes at 10 kHz. During the on-time the switching frequency is 208 kHz. As seen, transistors turn on at zero voltage. The experimental results show the application to machining operations performed on a carbon steel workpiece. The graphite electrode had negative polarity and the machining frequency was 10 kHz with a 50% duty cycle.

The dielectric fluid was tap-water-flushed by a jet directed against the gap. Fig. 7 shows gap voltage and current waveforms of effective discharges. During the on-time the output current is around 11 A and the output voltage is ∼30 V.

5. Nuclear power plant application

The EDM impulse generator has been validated to perform operations in a nuclear power plant application as is described below. The objective was to cut alignment pins. Three techniques were evaluated to perform the underwater operation:

- traditional machining by means of an abrasive wheel;
- metal disintegration machining (MDM);
- electrical discharge machining.

Specific machine tools were designed for each technique to perform the operation. The pin material is 304 stainless steel and their size is 22 mm Ø and 60 mm long. The EDM power supply is the prototype of the full-bridge series–parallel resonant converter. Voltage pulses are applied between the electrode and the workpiece at 10 kHz and the pulse width of the discharge is 25 μs. The electrode is flat and 2 mm thick, the electrode material is POCO EDM-100 graphite. The chosen electrode polarity is negative. The resulting cuts are shown in Fig. 8. The workpiece of Fig. 8(a) was cut by a manual operated saw with abrasive wheel and achieved the specified tolerance. The cut shown in Fig. 8(b) was performed by an MDM process. In the metal disintegration machining process a constant voltage supply and a vibrating head generate the machining pulses. Discharges take place when the electrode is close enough to the workpiece before they make physical contact. Electronics in MDM are very simple compared to EDM but the degree of control of MRR, SF and EW is lower. As shown in Fig. 8(b) the resulting surface finish is rough. This cut

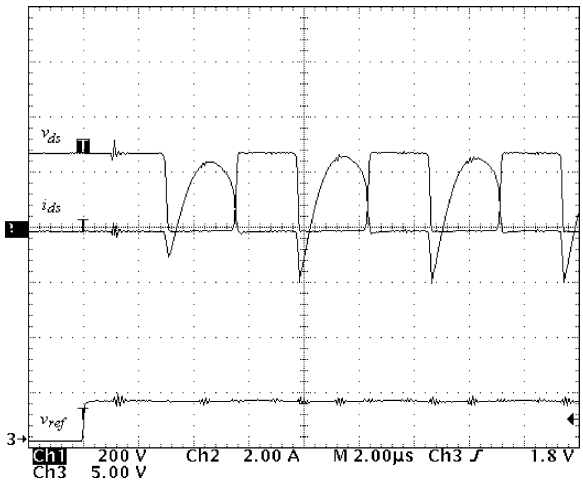

Fig. 6. Switching current and voltage.

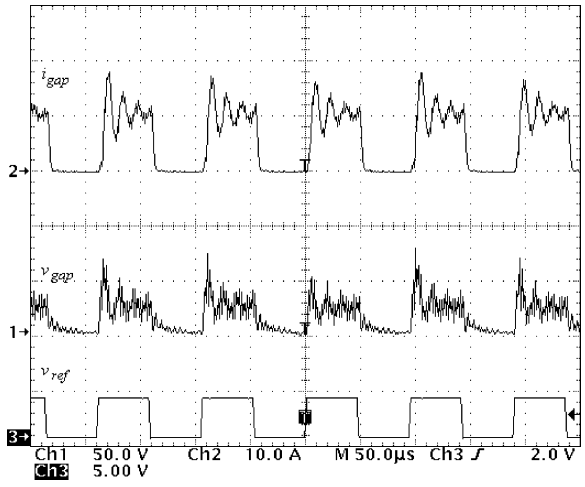

Fig. 7. Gap current and voltage.

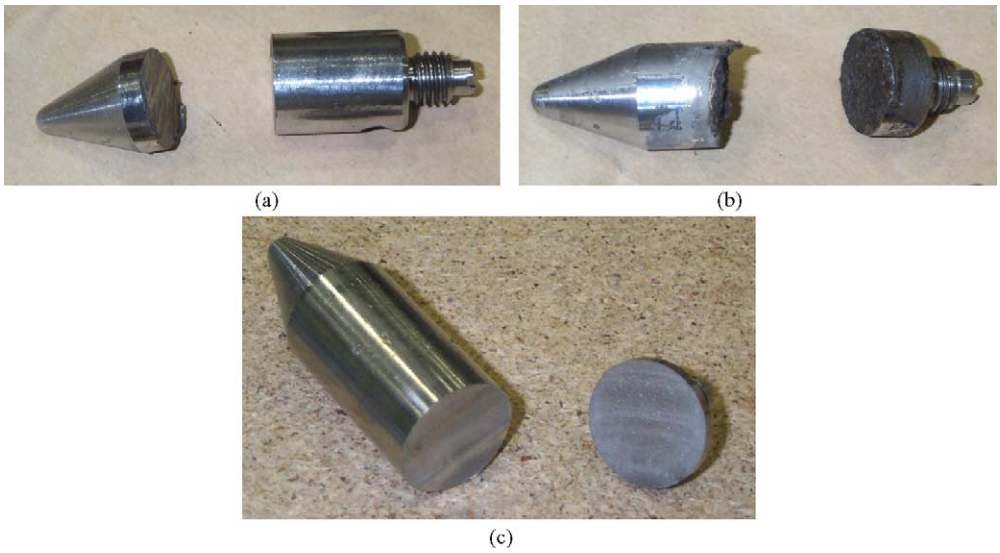

Fig. 8. Resulting cuts: (a) abrasive wheel, (b) MDM and (c) EDM.

needed four operations to be finished. The cut made with the proposed EDM system, Fig. 8(c), achieved the specified tolerance and the task of the operator was simply process surveillance.

6. Conclusions

A new EDM impulse generator based on a series–parallel resonant converter has been proposed resulting in a great reduction in weight and size, being especially suitable for portable operations. This technology, firstly oriented to underwater operations in nuclear plants, might be extended for chip-less metal machining at low cost. The design specifications of a series–parallel resonant converter for an EDM application have been established. The design strategy imposes a nominal operating point where the converter behaves as a current source. Current mode operation allows the increase of the output power as needed by connecting the necessary power cells in parallel as well as the reduction of the output ripple by interleaving the control of the cells.

The EDM impulse generator has been validated to perform operations in a nuclear power plant application. A comparative analysis with other alternative technologies demonstrates that the proposed EDM system achieves higher controllability and tighter tolerance in a practical cutting process.

Acknowledgements

This work has received financial support from the Spanish Government in the framework of the project CICYT DPI2001-1047.

References

[1] M.S. McGough, Advanced repair, modification and metallurgical sampling techniques for aging management of nuclear power plant components, Presented at the International Power Generation Conference, ASME Paper No. 91-IPGC-NE-29, 1991.
[2] T. Ikegami, T. Shimura, M. Koike, Plant life management and maintenance technologies for nuclear power plants, Hitachi Rev. 50 (3) (2001).
[3] T.L. Brown, et al., Combustion Engineering, US Patent 4 804 814 (1989).
[4] J.E. Hydeman, et al., Westinghouse Electric Corp., US Patent 5 543 599 (1996).
[5] M. Robergeau, General Electric, US Patent 6 233 301 (2001).
[6] H. Obara, T. Ohsumi, M. Hatano, Development of twin-type resistorless power supply for electrical discharge machining, in: Proc. of the ISEM XIII, 2001, pp. 153–160.
[7] G. Wollenberg, F. Luhn, A. Görisch, Pulsed EDM generators as sources of electromagnetic emission, in: Proc. of the ISEM XII, 1998, pp. 229–308.
[8] M.K. Kazimierczuk, D. Czarkowski, Resonant Power Converters, Wiley/Interscience, New York, 1995.
[9] R.L. Steigerwald, A comparison of half-bridge resonant converter topologies, IEEE Trans. Power Electron. 3 (2) (1988) 174–182.